The particle size effect of the spin-density wave in cubic γ-Fe precipitates in Cu

2004 J. Phys.: Condens. Matter 16 7723

(http://iopscience.iop.org/0953-8984/16/43/012)

INSTITUTE OF PHYSICS PUBLISHING JOURNAL OF PHYSICS: CONDENSED MATTER

J. Phys.: Condens. Matter **16** (2004) 7723–7732 PII: S0953-8984(04)82221-5

The particle size effect of the spin-density wave in cubic γ-Fe precipitates in Cu

Takaya Naono[1] **and Yorihiko Tsunoda**

School of Science and Engineering, Waseda University, 3-4-1 Ohkubo, Shinjuku, Tokyo, 169-8555, Japan

E-mail: tsunoda@waseda.jp

Received 17 June 2004, in final form 10 September 2004
Published 15 October 2004
Online at stacks.iop.org/JPhysCM/16/7723
doi:10.1088/0953-8984/16/43/012

Abstract

It is common knowledge that the magnetic structure of fcc Fe (γ-Fe) can be described by means of an incommensurate spin-density wave (SDW). Previous experimental data, however, were mostly obtained for γ-FeCo alloy precipitates in Cu in order to avoid the complexity of the structural phase transition. Since Fe is a fundamental element, reliable data on the SDW state for pure γ-Fe are highly desired. We present here neutron scattering data for the SDW in pure γ-Fe precipitates in Cu and discuss the particle size effect of the SDW.

1. Introduction

The magnetic structure of pure Fe in an fcc structure (γ-Fe) was first studied by Abrahams *et al* using γ-Fe precipitates in a Cu matrix, by means of neutron scattering experiments [1]. They reported it to be a longitudinal-type 1 antiferromagnetic (L-type 1 AF) structure with an inclined spin angle of about 19° from the *c*-axis. This structure was supported by the experimental data on γ-Fe alloys (FeMn and FeNiCr) which also showed the L-type 1 AF structure [2]. Thus, the magnetic structure of γ-Fe had long been believed to be an L-type 1 AF structure. In 1980, however, Ehrhart *et al* found a reduction of the fcc lattice symmetry of γ-Fe precipitates in Cu at the onset of antiferromagnetic order at low temperature [3]. One of the present authors studied the lattice and magnetic structures of γ-Fe precipitates more thoroughly using x-ray and neutron diffractions. Below the transition temperature, the crystal lattice is described in terms of a periodic shear wave propagating along the [1 1 0] direction with the $\langle 1\bar{1}0\rangle$ polarization vector [4]. Thus, the magnetic structure previously reported for the γ-Fe precipitates was not for the cubic γ-Fe but for the state with periodic lattice distortion. Careful examination of neutron scattering measurements revealed that the magnetic structure

[1] Present address: Instrumentation Engineering Division, Toyota Motor Corporation, 1 Toyota-cho, Toyota, Aichi, 471-8571, Japan.

of γ-Fe precipitates is a complex one which reflects the lattice structure realized below the structural phase transition temperature [5]. These results compelled the author (YT) to study the magnetic structure of γ-Fe in a cubic state. He found that the structural phase transition of γ-Fe precipitates at low temperature is suppressed for small size precipitates and/or by the introduction of a small amount of Co and the lattice retains a cubic structure even at the lowest temperature. Neutron scattering measurements for cubic γ-Fe revealed that the magnetic structure of cubic γ-Fe can be described in terms of an incommensurate spin-density wave (SDW) propagating along the [0 1 0] direction [6]. Nowadays, the SDW ground state of cubic γ-Fe is supported by various theories [7]. However, previous experimental data for the SDW in cubic γ-Fe were mostly obtained using the γ-FeCo alloy precipitates in Cu [6, 8] to avoid the complexity of the structural phase transition for larger size precipitates [9]. Since Fe is a fundamental element, reliable data on the SDW in pure γ-Fe are highly desired. In the present paper, we report on the particle size dependence of the SDW state in cubic γ-Fe precipitates in Cu using better statistical data obtained with a large specimen. The cubic γ-Fe precipitates with smaller particle size show the SDW with longer wavelength and higher Néel temperature. However, these values are constant for the precipitates with sizes between 20 and 40 nm diameter. The SDW structure is destroyed for precipitates larger than 40 nm due to the structural phase transition. The difference from the γ-FeCo precipitates is discussed.

2. Sample preparation and measurements

A supersaturated CuFe alloy with the Fe concentration of 2.8 at.% was melted in an induction furnace in advance; then a single crystal of the alloy with a volume of about 13 cm^3 was grown by the Bridgman method in an Ar atmosphere. After annealing to achieve homogenization at 1313 K for 24 h, the single crystal was quenched in water. The annealing to grow precipitates was performed at 848 K for various periods, so as to obtain the various target sizes of the precipitates. Susceptibility and neutron scattering measurements were performed at the each stage of annealing; then additional annealing was carried out to achieve growth to the next particle size. The averaged particle sizes of the precipitates were estimated by means of the equation reported by Borrelly *et al* [10] using the total annealing period. The target particle sizes presented here were the as-quenched size and 5, 10, 20, 40 and 80 nm in diameter. The particle sizes of the precipitates will be distributed about the mean value with the distribution function derived by Lifshitz and Wagner. In this paper, however, we refer to each specimen using the mean diameter of the precipitates—10 nm sample, 20 nm sample etc. After the each stage of annealing, the specimen was heavily etched in dilute nitric acid; then susceptibility and neutron scattering measurements were performed.

The susceptibility was measured using a SQUID system at the Materials Characterization Central Laboratory in Waseda University in a magnetic field of 100 Oe. For the susceptibility measurements, a small piece was cut off from the large single crystal for the neutron scattering experiments and the heat treatments for the small piece were always performed together with that of the large single crystal. Measurements were made for both field cooled (FC) and zero-field cooled (ZFC) processes.

Neutron scattering measurements were performed at the T1-1 triple-axis spectrometer installed at a thermal guide of JRR-3M, Tokai. Although we used a thick pyrolytic graphite filter to eliminate the higher order contamination, $(\lambda/2)(2\ 0\ 0)$ and $(\lambda/2)(2\ 2\ 0)$ Bragg peaks of Cu host were still observed at the (1 0 0) and (1 1 0) reciprocal lattice points, respectively, due to the large volume fraction of the Cu host.

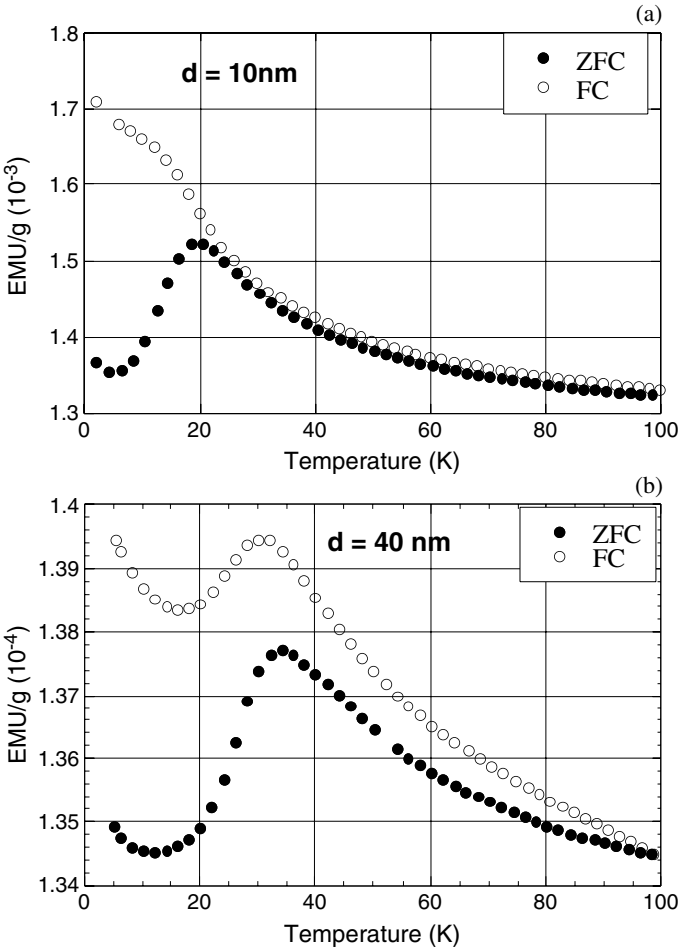

Figure 1. Susceptibility data for (a) the 10 nm sample and (b) the 40 nm sample studied under the field of 100 Oe.

3. Experimental data

3.1. Magnetic susceptibility

The susceptibility was measured at each stage of the annealing using a small sample cut from the single crystal for neutron scattering measurements. In figure 1, experimental data for the 10 and 40 nm samples are given, as typical patterns. Up to the 20 nm sample, the susceptibility data show a pattern very similar to those for typical spin-glass alloys: there is a cusp-type anomaly at the *spin freezing temperature* below which the FC and ZFC data trace different paths. The *spin freezing temperature* increases with increasing particle size. However, for the 40 and 80 nm samples, the FC data show a different path to the ZFC data over the whole temperature range of the measurements. The cusp-type anomaly still exists and the cusp temperature increases with increasing particle size even beyond 20 nm.

3.2. Neutron scattering

It is well known that the γ-Fe precipitates in Cu are spherical in shape. Although the lattice parameter of the γ-Fe precipitates is slightly smaller ($\sim$0.7%) than that of the Cu matrix, their

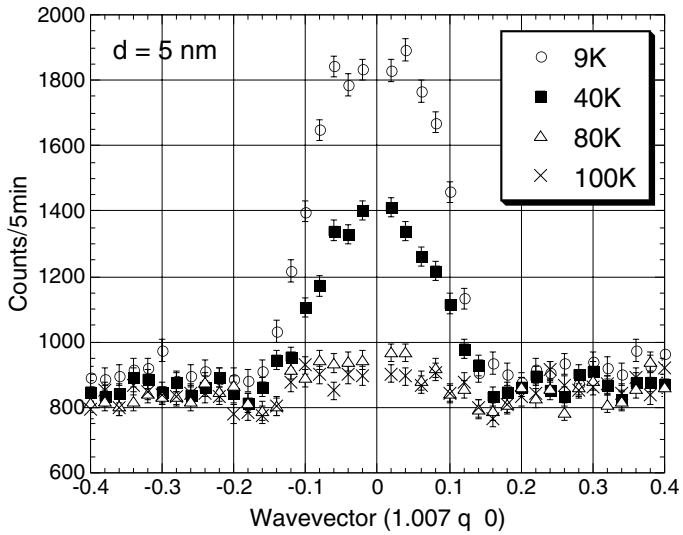

Figure 2. Temperature variations of the neutron scattering line profiles obtained for the 5 nm sample.

lattices are coherent with the Cu host. Thus the crystal axes of the precipitates are parallel to those of Cu. Since we used a single crystal of the Cu(Fe) specimen, all of the coherent γ-Fe precipitates have parallel cubic axes and we can observe the Bragg peaks of the γ-Fe precipitate on the common axes on the scattering plane as if it were a single crystal of γ-Fe. In this paper, we refer to the reciprocal lattice frame of the Cu matrix. Thus, the reciprocal lattice point (RLP) 1 0 0 of the γ-Fe precipitates is written as 1.007 0 0.

In the previous measurements, we knew that there were no magnetic peaks on the [1 0 0] axis. Thus, all of the present neutron scattering data were taken by scanning along the [0 1 0] direction passing through the 1.007 0 0 RLP. Although we started measurements for the as-quenched sample, for which we expected all of the Fe atoms to be isolated, a magnetic diffuse peak was observed at the 1.007 0 0 RLP, indicating that Fe clusters were already growing in the sample. Since the sample volume was quite large ($\sim$13 cm^3), it took a few seconds to cool the sample to room temperature in the quenching and clustering of Fe atoms started in the course of quenching.

In figure 2, an experimental line profile is given for the sample with the precipitate particle size 5 nm in diameter (5 nm sample), at several temperatures. Note that the diffraction pattern is composed of twin peaks. The temperature variation of the intensity at the maximum peak position is given in figure 3. The peak disappears at around 90 K, which is far higher than the cusp temperature in the susceptibility data. The data for the as-quenched sample were very similar to those for the 5 nm sample.

Typical satellite peaks of the SDW were obtained for the 20 nm sample. The line profiles and the temperature variation of the 1.007 δ 0 satellite peak for the 20 nm sample are given in figure 4. In this figure, the data at 80 K were subtracted to obtain the magnetic component.

The diffraction patterns obtained by scanning along the [0 1 0] direction passing through the 1.007 0 0 RLP for all specimens studied at 10 K are shown in figure 5. For the 80 nm sample, the satellite peaks disappear and the broad peak appears at the 1.007 0 0 RLP. The data for the 40 nm sample are described as sums of the satellite peaks and the broad peak centred at 1.007 0 0. The temperature variations of the satellite peak intensities are given in figure 6 for

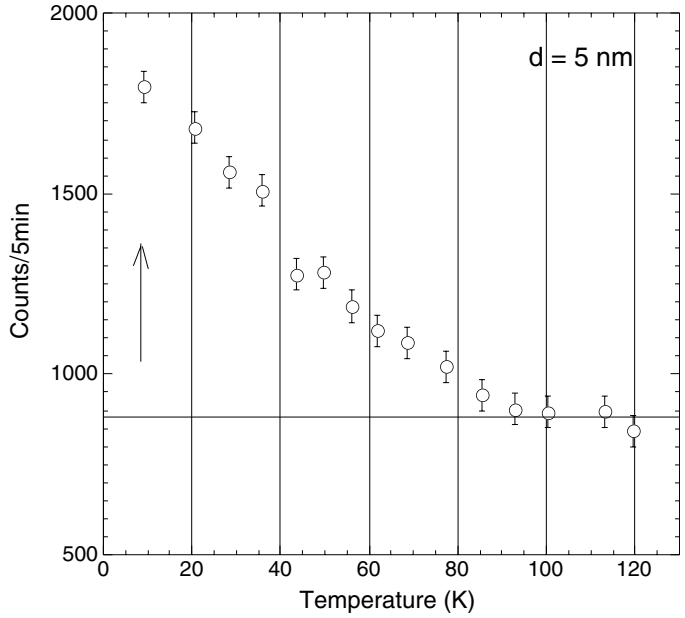

Figure 3. Temperature variations of the maximum peak intensity for the 5 nm sample. The arrow indicates the temperature at which the susceptibility data show an anomaly.

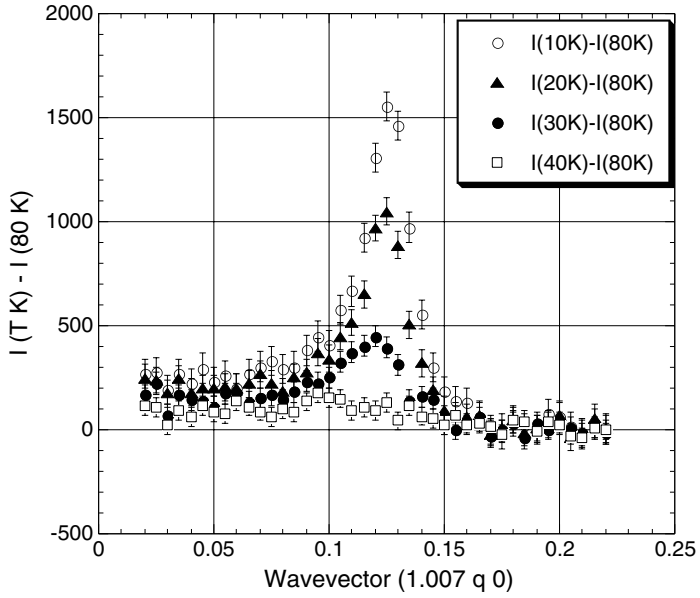

Figure 4. Temperature variations of the 1.007 δ 0 satellite peak for the 20 nm sample.

various particle sizes. The Néel temperature for small precipitates is higher than that for large precipitates and the value saturates to 40 K at the 20 nm sample. The satellite peak positions determined at 10 K are plotted in figure 7 as a function of particle size. The wavelength of the SDW depends crucially on the size of the precipitates. The small precipitates have a small δ value (long wavelength) and the wavelength again saturates to $\lambda = 2.5$ nm ($\delta = 0.127$ (units of $2\pi/a$)) at around the 20 nm sample.

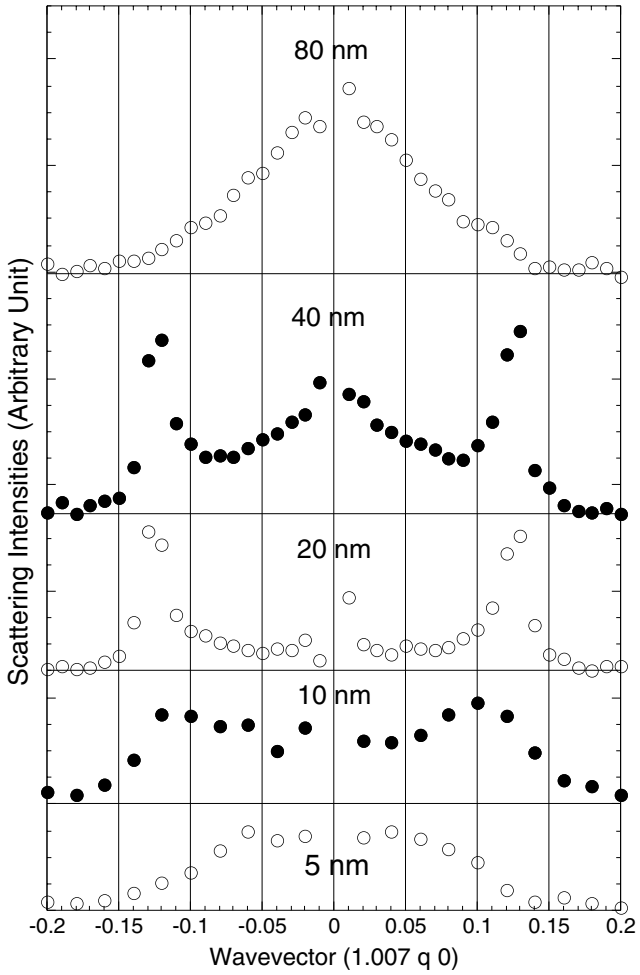

Figure 5. Line profiles for all samples obtained at 10 K by scanning along the [0 1 0] axis passing through the 1.007 0 0 RLP.

4. Discussion

4.1. Susceptibility

The spin-glass properties of rapidly quenched CuFe alloys were reported by Adachi *et al* [11]. Our susceptibility data showed a cusp-type anomaly for all of the samples and the cusp temperature increased with increasing particle size. The Néel temperature of the SDW determined by neutron scattering however behaves in a completely opposite way to that for the small precipitates: the satellite peak disappears at around 90 K for the 5 nm sample and the Néel temperature decreases with increasing particle size, then reaches a stable value $T_N = 40$ K for the 20 nm sample. For the small precipitates, the discrepancy could be understood as reflecting a superparamagnetic behaviour of the SDW. Inside the precipitates, the SDW orders at high temperature, but behaves superparamagnetically via thermal fluctuations. Since the characteristic frequency of the neutron scattering is very high ($\sim 10^{11}$ Hz), we can observe the SDW magnetic ordering inside the precipitates by means of neutron scattering at rather high temperature. However, no anomaly is observed in the susceptibility data at the Néel temperature. This is consistent with the Mössbauer spectroscopy data reported by

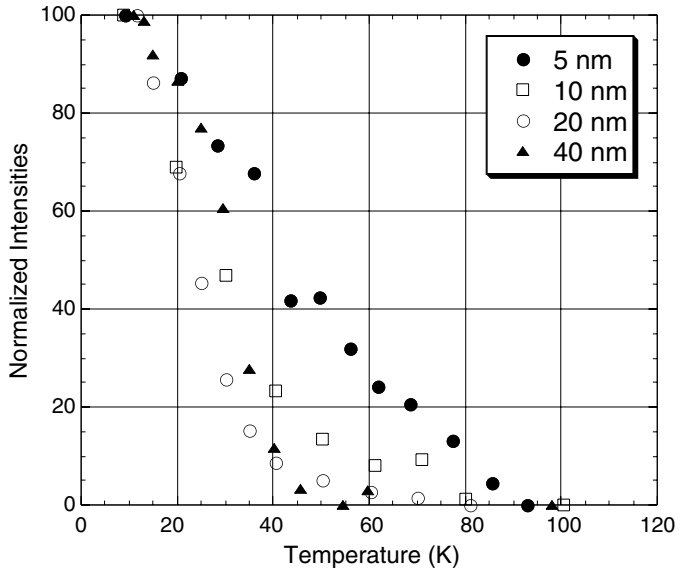

Figure 6. Temperature variations of the satellite peak intensities for the various samples.

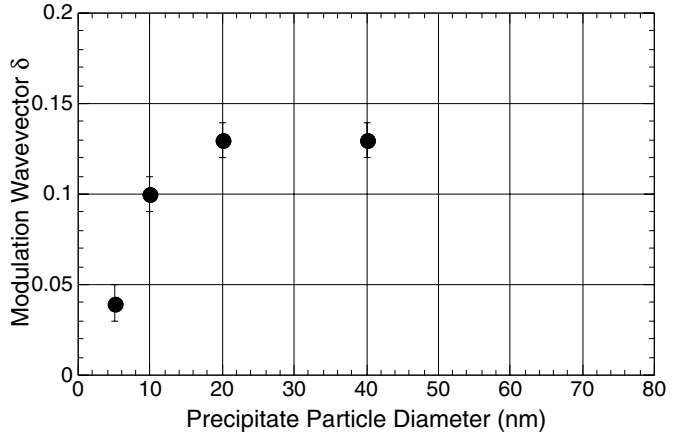

Figure 7. The particle size dependence of the wavevector of the SDW in pure γ-Fe precipitates.

Ezawa *et al* [12]. For small precipitates ($d < 20$ nm), the Néel temperature determined by Mössbauer spectroscopy decreases with decreasing particle size and shows an intermediate value between neutron and susceptibility data. Since the characteristic frequency of Mössbauer spectroscopy is about $\sim 10^7$ Hz, the freezing of the superparamagnetic fluctuation is observed at lower temperature than that for neutron scattering. Then, the susceptibility anomaly should correspond to the freezing of the superparamagnetic SDW for small precipitates. In the present case, however, the specimens show more complex features. The system always includes a non-negligible amount of isolated Fe moments (ppm order) even in the growth process of the precipitates. The system with large precipitates includes a small amount of bcc Fe (α-Fe) precipitates, which is very sensitive to the magnetization data. Then, we have to consider various contributions to the magnetization data.

(1) The spin freezing between the isolated Fe moments which couple through the RKKY interaction.
(2) The magnetic ordering of Fe moments inside the γ-Fe precipitates.

(3) The freezing between the γ-Fe precipitate particles.
(4) The coupling between the isolated Fe moments and the ordered SDW in γ-Fe precipitates.
(5) The magnetization of ferromagnetic α-Fe particles for the system with large precipitates.

Furthermore, we have to consider that the effective concentrations of the isolated Fe and γ-Fe precipitates would change in each step of the ageing process. The magnetization data reflect all of these magnetic behaviours, while in neutron scattering measurements we observe only the magnetic ordering of (2). Since the cusp-type anomalies of the susceptibility data do not correspond to the Néel temperature determined by means of neutron scattering, our magnetization data are not a direct reflection of the magnetism inside the γ-Fe precipitates. It is considered that the anomalies in the susceptibility data could be a reflection of any of the freezing processes listed in (1), (3) and (4) and they are beyond the scope of the present paper. The susceptibilities for the samples with various particle sizes of γ-Fe precipitates remain as future problems.

4.2. Neutron scattering

Various properties observed here for the SDW in pure γ-Fe precipitates are very similar to those previously reported for γ-$Fe_{97}Co_3$ alloy precipitates [8]. The SDW in small precipitates has long wavelength and shows a high Néel temperature. The stable values of the wavelength and the Néel temperature for the SDW in pure γ-Fe precipitates are 2.5 nm ($\delta = 0.127$ (units of $2\pi/a$)) and ~40 K, respectively, and are obtained for precipitates larger than 20 nm in diameter. The Néel temperature for pure γ-Fe being slightly higher than that for the γ-$Fe_{97}Co_3$ precipitates is an alloying effect of Co ($T_N \sim 30$ K for γ-$Fe_{97}Co_3$ precipitates). This is reasonable because the Néel temperature of the SDW decreases with increasing Co concentration and disappears around γ-$Fe_{92}Co_8$ alloy precipitates [9].

The marked difference between the γ-Fe and γ-$Fe_{97}Co_3$ precipitates is the disappearance of the SDW satellite peaks for the large γ-Fe precipitates. This is due to the structural phase transition which is observed in the large γ-Fe precipitates, but is suppressed for the γ-$Fe_{97}Co_3$ alloy precipitates of any size. The reason that the structural phase transition is suppressed for γ-FeCo precipitates is still unknown. One possible explanation is a lattice contraction of FeCo alloy precipitates in Cu. The relative value of the lattice spacing a(precipitate)/a(Cu) for γ-$Fe_{90}Co_{10}$ precipitates is 0.9916 at 10 K, while that for γ-Fe precipitates is 0.9928, indicating that the mismatch of the lattices between precipitates and the Cu host is larger for the γ-FeCo precipitates [13]. Thus, the γ-FeCo precipitates suffer a stronger expansion force which suppresses the structural phase transition.

The structural phase transition destroys the SDW of γ-Fe and induces a new magnetic structure which reflects the lattice structure at the low temperature phase of the γ-Fe precipitates. The magnetic structure of γ-Fe under the influence of the periodically distorted lattice below the structural phase transition temperature (T_t) was reported in detail in the previous paper [5]. The result was completely different from that reported by Abrahams *et al* [1] but we do not repeat the result here. The 1 0 0 diffuse peak observed for the 80 nm sample is explained as the transverse spin component of the low temperature spin structure below T_t and was minutely discussed in the previous paper [14]. In figure 8, the 1 1 0 magnetic peak intensity contour map is given for the 80 nm sample. The intensity map elongates along the cubic axes and this pattern is also well explained by the magnetic structure under the influence of the periodic lattice distortion [5]. For the 40 nm sample, the SDW satellite peaks and the 1 0 0 diffuse peak coexist, indicating the coexistence of cubic γ-Fe and the periodically distorted γ-Fe precipitates. These results are again consistent with the Mössbauer spectroscopy data reported by Ezawa *et al* [12].

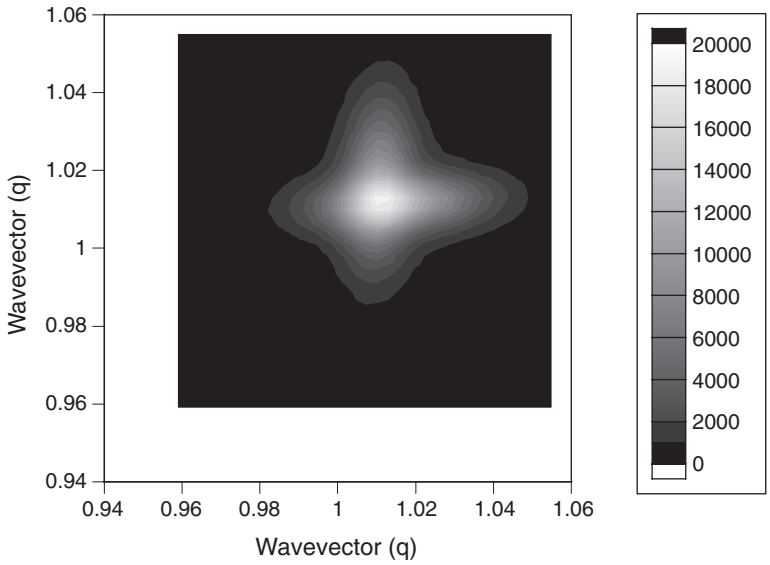

Figure 8. The (1 1 0) magnetic peak intensity contour map studied for the 80 nm sample.

The γ-Fe precipitates smaller than 20 nm in diameter show a higher Néel temperature and smaller modulation wavevector δ of the SDW. These are considered to be due to the effect of the Cu host. The influence of the Cu host on the small γ-Fe precipitates is also observed in the phonon density of states (DOS) studied by means of nuclear resonant inelastic scattering of synchrotron radiation [15] and the effect extends up to about 15 nm precipitates. The influence of the Cu host on the small γ-Fe precipitates is considered to be twofold. Since the stable value of the lattice spacing of γ-Fe is slightly ($\sim$0.7%) smaller than that of the Cu host, smaller precipitates suffer a stronger expansive force because of the relatively large surface fraction. Thus, the smaller precipitates have slightly larger lattice spacing than the stable value [16]. If the negative pressure for the small precipitates is the origin of the high Néel temperature and small δ value of the SDW, a positive high pressure should decrease the Néel temperature and increase the δ value. Mössbauer spectroscopy data for γ-Fe precipitates in Cu under high pressure were reported for a sample with 6 nm precipitates and the results indeed show a decrease of the Néel temperature with the rate of -5 K GPa^{-1} [17]. If we apply this value to the present case, 5 and 10 nm precipitates suffer negative pressure of about 10 and 3.5 GPa, respectively. There are no data on the modulation wavevector δ of the SDW under high pressure.

Another possible influence of the Cu host on the small precipitates is that of direct inflow (outflow) of electrons through the interfaces. Since the introduction of a small amount of Co strongly suppresses the Néel temperature, the SDW state of the γ-Fe precipitates would be very sensitive to the electronic configuration. However, the experimental data have a special feature. Although the linewidth of the satellite peaks is very broad for small precipitates, the satellite peak is a single peak, indicating that the effect of the host metal extends over the whole volume of the small precipitates. Thus, if the direct inflow (outflow) of electrons is the origin of the size effect of the SDW, we have to consider the influence to extend over the whole volume of the small precipitates.

The satellite peak line shape is asymmetric even for the 20 nm sample, for which most of the precipitates retain the cubic structure. This is explained by the distribution of the particle sizes. The large precipitates show a stable value of the SDW wavevector δ, while the smaller

precipitates have smaller δ values which depend on the particle sizes. Thus, the asymmetric line shape of the satellite peak results.

We tried to determine the magnetic moment of the SDW in γ-Fe from the intensity ratio of magnetic to nuclear scattering. It was however impossible to separate the nuclear Bragg peak of γ-Fe precipitates from that of the Cu host due to the poor resolution of the neutron scattering experiment. This remains as a future problem.

The possibility of a multiple-Q SDW state is theoretically proposed [18] as a ground state for cubic γ-Fe. In neutron scattering experiments, it is impossible in principle to distinguish the multiple-Q SDW state and the single-Q SDW state with multiple Q domains if the system has a cubic structure and the Q domains distribute equally. The γ-Fe precipitates in Cu are these cases. The satellite peak intensities studied under uniaxial stress along the cubic axis, however, show strong anisotropic distribution [19]; the satellite peak intensities located on the axis along the uniaxial stress direction drastically increase, indicating that the SDW favours the single-Q state at least under uniaxial stress. The experimental data may suggest that cubic γ-Fe slightly contracts along the modulation wavevector direction at the onset of the SDW, although the magnitude of the contraction is too small to be observed.

In the present paper, neutron scattering and susceptibility data for pure γ-Fe precipitates in Cu were reported for various particle sizes. The anomaly of the susceptibility data did not reflect the Néel temperature of the SDW in the γ-Fe precipitates. The SDW in the smaller precipitates has longer wavelength and higher Néel temperature, probably due to the larger lattice spacing under the strong expansive force. The stable values of the wavelength and the Néel temperature of the SDW in pure γ-Fe are 2.5 nm ($\delta = 0.127$ (units of $2\pi/a$)) and 40 K, respectively, and were obtained for the precipitates with diameter in the range 20 nm $< d <$ 40 nm. For the precipitates larger than 40 nm diameter, the structural phase transition takes place and the SDW structure of γ-Fe is destroyed.

References

[1] Abrahams S C, Guttman L and Kasper J S 1962 *Phys. Rev.* **127** 2052–5
[2] Endoh Y and Ishikawa Y 1971 *J. Phys. Soc. Japan* **30** 1614–27
Ishikawa Y, Kohgi M and Noda Y 1975 *J. Phys. Soc. Japan* **39** 675
[3] Ehrhart P, Schonfeld B, Ettwig H H and Pepperhoff W 1980 *J. Magn. Magn. Mater.* **22** 79–85
[4] Tsunoda Y and Kunitomi N 1988 *J. Phys. F: Met. Phys.* **18** 1405–12
[5] Tsunoda Y, Kunitomi N and Nicklow R M 1987 *J. Phys. F: Met. Phys.* **17** 2447–58
[6] Tsunoda Y 1988 *J. Phys. F: Met. Phys.* **18** L251–5
[7] Knöpfle K, Sandratskii L M and Kübler J 2000 *Phys. Rev.* B **62** 5564–9
Kleinman L 1999 *Phys. Rev.* B **59** 3314
Bylander D M and Kleinman L 1999 *Phys. Rev.* B **60** R9916–8
Uhl M, Sandratskii L M and Kübler J 1992 *J. Magn. Magn. Mater.* **103** 314–24
Mryasov O N, Gubanov V A and Liechtenstein A I 1992 *Phys. Rev.* B **45** 12330–6
Hirai K 1989 *J. Phys. Soc. Japan* **58** 4288
[8] Tsunoda Y 1990 *Prog. Theor. Phys. Suppl.* **101** 133–8
[9] Tsunoda Y 1989 *J. Phys.: Condens. Matter* **1** 10427–38
[10] Borrelly R, Pelletier J M and Pernoux E 1975 *Scr. Metall.* **9** 747–52
[11] Adachi K, Uchiyama T, Matsui M, Doi M and Miyazaki T 1986 *J. Magn. Magn. Mater.* **54–57** 115
[12] Ezawa T, Macedo W A A, Glos U, Keune W, Schletz K P and Kirschbaum U 1989 *Physica* B **161** 281–4
[13] Tsunoda Y, unpublished work
[14] Tsunoda Y and Nicklow R M 1993 *J. Phys.: Condens. Matter* **5** 8999–9008
[15] Tsunoda Y, Kurimoto Y, Seto M, Kitao S and Yoda Y 2002 *Phys. Rev.* B **66** 214304
[16] Tsunoda Y, Imada S and Kunitomi N 1988 *J. Phys. F: Met. Phys.* **18** 1421–31
[17] Liu C M and Ingalls R 1979 *J. Appl. Phys.* **50** 1751
[18] Kakehashi Y and Kimura N 1999 *Phys. Rev.* B **60** 3316
Uchida T and Kakehashi Y 2003 *Phys. Status Solidi* a **196** 193–6
[19] Nogami H and Tsunoda Y, unpublished work